REPORT DOCUMENTATION PAGE

Form Approved OMB NO. 0704-0188

1. REPORT DATE (DD-MM-YYYY)	2. REPORT TYPE	3. DATES COVERED (From - To)
16-11-2019	Final Report	1-May-2016 - 30-Sep-2019

4. TITLE AND SUBTITLE
Final Report: Hyperbolic Reconstructed-Discontinuous-Galerkin Method for Accurate Unsteady Viscous Simulations on Unstructured Grids

5a. CONTRACT NUMBER
W911NF-16-1-0108

5b. GRANT NUMBER

5c. PROGRAM ELEMENT NUMBER
611102

6. AUTHORS

5d. PROJECT NUMBER

5e. TASK NUMBER

5f. WORK UNIT NUMBER

7. PERFORMING ORGANIZATION NAMES AND ADDRESSES
National Institute of Aerospace Associates
100 Exploration Way

Hampton, VA 23666 -6186

8. PERFORMING ORGANIZATION REPORT NUMBER

9. SPONSORING/MONITORING AGENCY NAME(S) AND ADDRESS (ES)
U.S. Army Research Office
P.O. Box 12211
Research Triangle Park, NC 27709-2211

10. SPONSOR/MONITOR'S ACRONYM(S)
ARO

11. SPONSOR/MONITOR'S REPORT NUMBER(S)
68765-EG.19

12. DISTRIBUTION AVAILIBILITY STATEMENT
Approved for public release; distribution is unlimited.

13. SUPPLEMENTARY NOTES
The views, opinions and/or findings contained in this report are those of the author(s) and should not contrued as an official Department of the Army position, policy or decision, unless so designated by other documentation.

14. ABSTRACT

15. SUBJECT TERMS

16. SECURITY CLASSIFICATION OF:			17. LIMITATION OF ABSTRACT	15. NUMBER OF PAGES	19a. NAME OF RESPONSIBLE PERSON
a. REPORT	b. ABSTRACT	c. THIS PAGE			Hiroaki Nishikawa
UU	UU	UU	UU		19b. TELEPHONE NUMBER 757-864-7244

RPPR Final Report
as of 07-Jan-2020

Agency Code:

Proposal Number: 68765EG **Agreement Number: W911NF-16-1-0108**
INVESTIGATOR(S):

Name: Hiroaki Nishikawa
Email: hiro@nianet.org
Phone Number: 7578647244
Principal: Y

Organization: **National Institute of Aerospace Associates**
Address: 100 Exploration Way, Hampton, VA 236666186
Country: USA
DUNS Number: 114054443 EIN: 542065665
Report Date: 31-Dec-2019 Date Received: 16-Nov-2019
Final Report for Period Beginning 01-May-2016 and Ending 30-Sep-2019
Title: Hyperbolic Reconstructed-Discontinuous-Galerkin Method for Accurate Unsteady Viscous Simulations on Unstructured Grids
Begin Performance Period: 01-May-2016 **End Performance Period:** 30-Sep-2019
Report Term: 0-Other
Submitted By: Hiroaki Nishikawa Email: hiro@nianet.org
Phone: (757) 864-7244
Distribution Statement: 1-Approved for public release; distribution is unlimited.

STEM Degrees: 3 **STEM Participants:** 0

Major Goals: Milestone 1: Upon completion of the first three tasks, we will have a Hyp-rDG method to solve scalar convection-diffusion equation on hybrid grids. The performance of the Hyp-rDG method will be assessed in comparison with conventional methods. The advantages of the Hyp-rDG method will be demonstrated for a model convection-diffusion equation by (1) convergence acceleration, at least, in diffusion dominated cases and (2) high-order and high-quality derivative prediction on highly irregular grids. Successful demonstration will greatly encourage the extension to the compressible NS equations. --- COMPLETED in YEAR 1 as planned.

Milestone 2: Upon completion of this task, we will have a Hyp-rDG method that allows us to conduct accurate, efficient, and robust 1D, 2D, and 3D simulations for compressible viscous flows on hybrid grids. Upon completion of the tasks 4-6, we will have a Hyp-rDG method to solve the compressible Navier-Stokes equations on hybrid grids. The performance of the Hyp- rDG method will be assessed in comparison with conventional methods. The advantages of the Hyp-rDG method will be demonstrated for a variety of viscous flow problems by (1) convergence acceleration, at least, in diffusion dominated cases and (2) high-order and high-quality derivative prediction on highly irregular grids. --- COMPLETED in YEAR 2 and 3 as planned.

Accomplishments: - Developed a systematic construction of efficient hyperbolic reconstructed discontinuous Galerkin schemes for model equations.

- Discovered that the hyperbolic reconstructed discontinuous Galerkin method can be time accurate with explicit time-stepping schemes.

- Demonstrated the hyperbolic method for diffusion problems with discon- tinuous coefficients as well as for tensor coefficients.

- Developed a new hyperbolic Navier-Stokes system (HNS20G) to enable an efficient high-order scheme construction.

- Derived an optimal length scale for improving the performance of the hy- perbolic method for high Reynolds number flows.

- Developed a weak formulation based on the primitive variables instead of the conservative variables.

- Demonstrated superior accuracy and efficiency of the hyperbolic recon- structed discontinuous Galerkin method for steady and unsteady viscous flow cases.

Training Opportunities: The project involved three graduate students at NCSU and provided training and professional development for them.

1. Xiaodong Liu worked on the project and published some papers. He gained experience in the algorithm development for unstructured-grid CFD methods through one-on-one work with the PI and the Co-PI. He graduated in the first year and currently works at Los Alamos National Laboratory.

2. Jialin Lou worked on the project for two years and published many papers. He gained experience in the algorithm development for unstructured-grid CFD methods through one-on-one work with the PI and the Co-PI. He graduated in the second year and currently works at Old Dominion University.

3. Lingquan Li worked on the project for the whole duration and published all papers. She gained experience in the algorithm development for unstructured-grid CFD methods through one-on-one work with the PI and the Co-PI. She graduated in October 2019.

Results Dissemination: All results have been disseminated through 5 journal publications (1 in Computer Physics Communications, and 4 in the prestigious Journal of Computational Physics), 12 conference papers and presentations at major AIAA conferences and an international conference. All publications were advertised through various SNS channels (e.g., twitter, LinkedIn, etc.). Lingquan Li presented the final results at the NIA CFD Seminar on 09-04-2019 and it was webcast to the whole world.

Honors and Awards: The PI (Hiroaki Nishikawa) was selected as the Engineer of the Year (AIAA Hampton Roads section) in September 2019, https://drive.google.com/file/d/1Makd65g9QBJzFyfs4RoGWY-xHYc_T3Hu/view

Protocol Activity Status:

Technology Transfer: Nothing to Report

PARTICIPANTS:

Participant Type: PD/PI
Participant: Hiroaki Nishikawa
Person Months Worked: 2.00 **Funding Support:**
Project Contribution:
International Collaboration:
International Travel:
National Academy Member: N
Other Collaborators:

Participant Type: Co PD/PI
Participant: Hong Luo
Person Months Worked: 2.00 **Funding Support:**
Project Contribution:
International Collaboration:
International Travel:
National Academy Member: N
Other Collaborators:

Participant Type: Graduate Student (research assistant)
Participant: Xiaodong Liu
Person Months Worked: 6.00 **Funding Support:**
Project Contribution:
International Collaboration:

International Travel:
National Academy Member: N
Other Collaborators:

Participant Type: Graduate Student (research assistant)
Participant: Jialin Lou
Person Months Worked: 10.00 **Funding Support:**
Project Contribution:
International Collaboration:
International Travel:
National Academy Member: N
Other Collaborators:

Participant Type: Graduate Student (research assistant)
Participant: Lingquan Li
Person Months Worked: 12.00 **Funding Support:**
Project Contribution:
International Collaboration:
International Travel:
National Academy Member: N
Other Collaborators:

CONFERENCE PAPERS:

Publication Type: Conference Paper or Presentation **Publication Status:** 1-Published
Conference Name: 55th AIAA Aerospace Sciences Meeting
Date Received: 03-Aug-2017 Conference Date: 09-Jan-2017 Date Published: 09-Jan-2017
Conference Location: Grapevine, Texas
Paper Title: Reconstructed Discontinuous Galerkin Methods for Diffusion Using a First-Order Hyperbolic System Formulation
Authors: Jialin Lou, Xiaodong Liu, Hong Luo, Hiroaki Nishikawa
Acknowledged Federal Support: **Y**

Publication Type: Conference Paper or Presentation **Publication Status:** 1-Published
Conference Name: 23rd AIAA Computational Fluid Dynamics Conference
Date Received: 03-Aug-2017 Conference Date: 05-Jun-2017 Date Published: 05-Jun-2017
Conference Location: Denver, Colorado
Paper Title: A Finite Volume Method Based on Variational Reconstruction for Compressible Flows on Arbitrary Grids
Authors: Lingquan Li, Xiaodong Liu, Jialin Lou, Hong Luo, Hiroaki Nishikawa, Yuxin Ren|
Acknowledged Federal Support: **Y**

Publication Type: Conference Paper or Presentation **Publication Status:** 1-Published
Conference Name: 23rd AIAA Computational Fluid Dynamics Conference
Date Received: 03-Aug-2017 Conference Date: 05-Jun-2017 Date Published: 05-Jun-2017
Conference Location: Denver, Colorado
Paper Title: Uses of Zero and Negative Volume Elements for Node-Centered Edge-Based Discretization
Authors: Hiroaki Nishikawa
Acknowledged Federal Support: **Y**

RPPR Final Report
as of 07-Jan-2020

Publication Type: Conference Paper or Presentation **Publication Status:** 1-Published
Conference Name: 23rd AIAA Computational Fluid Dynamics Conference
Date Received: 03-Aug-2017 Conference Date: 05-Jun-2017 Date Published: 05-Jun-2017
Conference Location: Denver, Colorado
Paper Title: Reconstructed Discontinuous Galerkin Methods Based on First-Order Hyperbolic System for Advection-Diffusion Equations
Authors: Jialin Lou, Lingquan Li, Xiaodong Liu, Hong Luo, Hiroaki Nishikawa
Acknowledged Federal Support: **Y**

Publication Type: Conference Paper or Presentation **Publication Status:** 1-Published
Conference Name: The 9th International Conference on Computational Fluid Dynamics
Date Received: 04-Aug-2017 Conference Date: 11-Jul-2016 Date Published: 11-Jul-2016
Conference Location: Istanbul, Turkey
Paper Title: Discontinuous Galerkin Methods for Hyperbolic Advection-Diffusion Equation on Unstructured Grids.
Authors: Jialin Lou, Hong Luo, and Hiroaki Nishikawa
Acknowledged Federal Support: **Y**

Publication Type: Conference Paper or Presentation **Publication Status:** 1-Published
Conference Name: AIAA Aerospace Sciences Meeting
Date Received: 03-Sep-2018 Conference Date: 08-Jan-2018 Date Published: 08-Jan-2018
Conference Location: Kissimmee, Florida
Paper Title: First-Order Hyperbolic System Based Reconstructed Discontinuous Galerkin Methods for Nonlinear Diffusion Equations on Unstructured Grids
Authors: Jialin Lou, Lingquan Li, Hong Luo, Hiroaki Nishikawa
Acknowledged Federal Support: **Y**

Publication Type: Conference Paper or Presentation **Publication Status:** 1-Published
Conference Name: AIAA Aerospace Sciences Meeting
Date Received: 03-Sep-2018 Conference Date: 08-Jan-2018 Date Published: 08-Jan-2018
Conference Location: Kissimmee, Florida
Paper Title: A Discontinuous Galerkin Method Based on Variational Reconstruction for Compressible Flows on Arbitrary Grids
Authors: Lingquan Li, Xiaodong Liu, Jialin Lou, Hong Luo, Hiroaki Nishikawa, Yuxin Ren
Acknowledged Federal Support: **Y**

Publication Type: Conference Paper or Presentation **Publication Status:** 1-Published
Conference Name: Fluid Dynamics Conference
Date Received: 03-Sep-2018 Conference Date: 08-Jan-2018 Date Published: 08-Jan-2018
Conference Location: Atlanta, Georgia
Paper Title: Explicit Hyperbolic Reconstructed Discontinuous Galerkin Methods for Time-Dependent Problems
Authors: Jialin Lou, Lingquan Li, Hong Luo, Hiroaki Nishikawa
Acknowledged Federal Support: **Y**

Publication Type: Conference Paper or Presentation **Publication Status:** 1-Published
Conference Name: Fluid Dynamics Conference
Date Received: 03-Sep-2018 Conference Date: 08-Jan-2018 Date Published: 08-Jan-2018
Conference Location: Atlanta, Georgia
Paper Title: A New Formulation of Hyperbolic Navier-Stokes Solver based on Finite Volume Method on Arbitrary Grids
Authors: Lingquan Li, Jialin Lou, Hong Luo, Hiroaki Nishikawa
Acknowledged Federal Support: **Y**

RPPR Final Report
as of 07-Jan-2020

Publication Type: Conference Paper or Presentation **Publication Status:** 0-Other
Conference Name: AIAA Scitech 2019 Forum
Date Received: 16-Nov-2019 Conference Date: 07-Jan-2019 Date Published: 07-Jan-2019
Conference Location: San Diego, California
Paper Title: High-Order Hyperbolic Navier-Stokes Reconstructed Discontinuous Galerkin Method
Authors: Lingquan Li, Jialin Lou, Hong Luo, and Hiroaki Nishikawa
Acknowledged Federal Support: **Y**

Publication Type: Conference Paper or Presentation **Publication Status:** 0-Other
Conference Name: AIAA Aviation 2019 Forum
Date Received: 16-Nov-2019 Conference Date: 17-Jun-2019 Date Published: 17-Jul-2019
Conference Location: Dallas, Texas
Paper Title: High-Order Hyperbolic Navier-Stokes Reconstructed Discontinuous Galerkin Method for Unsteady Flows
Authors: Lingquan Li, Jialin Lou, Hong Luo, and Hiroaki Nishikawa
Acknowledged Federal Support: **Y**

Publication Type: Conference Paper or Presentation **Publication Status:** 0-Other
Conference Name: 55th AIAA Aerospace Sciences Meeting
Date Received: 16-Nov-2019 Conference Date: 09-Jan-2017 Date Published: 09-Jan-2017
Conference Location: Grapevine, Texas
Paper Title: Hyperbolic Navier-Stokes Method for High-Reynolds- Number Boundary Layer Flows
Authors: H. Nishikawa and Y. Liu
Acknowledged Federal Support: **Y**

DISSERTATIONS:

Publication Type: Thesis or Dissertation
Institution: North Carolina State University
Date Received: 16-Nov-2019 Completion Date: 10/20/19 12:33PM
Title: Hyperbolic Navier-Stokes Method Based on Reconstructed-Discontinuous-Galerkin or Reconstructed-Finite-Volume Formulation with Variational Reconstruction
Authors: Lingquan Li
Acknowledged Federal Support: **N**

Hyperbolic Reconstructed-Discontinuous-Galerkin Method for Accurate Unsteady Viscous Simulations on Unstructured Grids (Final Report)

PI: Hiroaki Nishikawa, Co-PI: Hong Luo
Lingquan Li, Jialin Lou, Xiaodong Liu

November 2019

Summary

This report describes the research activities we have conducted at North Carolina State University (NCSU) and National Institute of Aerospace in fulfilling our contract (W911NF-16-1-0108) to the U.S. Army Research Office from May 2016 to September 2019. The technical progress of the work during the three years toward achieving the objectives of the proposed work is reported. The significant accomplishments are discussed. The hyperbolic reconstructed discontinuous Galerkin method is first implemented for model equations, and then applied to compressible Navier-Stokes equations. It is then extended to unsteady viscous simulations on unstructured grids. Numerical simulations are presented to illustrate the work performed. Conclusions and future work are discussed.

List of Accomplishments:

- Developed a systematic construction of efficient hyperbolic reconstructed discontinuous Galerkin schemes for model equations.

- Discovered that the hyperbolic reconstructed discontinuous Galerkin method can be time accurate with explicit time-stepping schemes.

- Demonstrated the hyperbolic method for diffusion problems with discontinuous coefficients as well as for tensor coefficients.

- Developed a new hyperbolic Navier-Stokes system (HNS20G) to enable an efficient high-order scheme construction.

- Derived an optimal length scale for improving the performance of the hyperbolic method for high Reynolds number flows.

- Developed a weak formulation based on the primitive variables instead of the conservative variables.

- Demonstrated superior accuracy and efficiency of the hyperbolic reconstructed discontinuous Galerkin method for steady and unsteady viscous flow cases.

List of Journal Publications (5):

J. Lou, X. Liu, H. Luo, and H. Nishikawa, Reconstructed Discontinuous Galerkin Methods for Hyperbolic Diffusion Equations on Unstructured Grids, Commun. Comput. Phys., 25, pp. 1302-1327, 2019

J. Lou, L. Li, H. Luo, and H. Nishikawa, "Reconstructed discontinuous Galerkin methods for linear advection-diffusion equations based on first-order hyperbolic system", Journal of Computational Physics, Volume 369, pp. 103-124, 2018.

H. Nishikawa and Y. Liu, Hyperbolic Advection-Diffusion Schemes for High-Reynolds-Number Boundary-Layer Problems, Journal of Computational Physics, Volume 352, pp. 23-51, 2018.

H. Nishikawa and Y. Nakashima, Dimensional Scaling and Numerical Similarity in Hyperbolic Method for Diffusion, Journal of Computational Physics, Volume 355, pp. 121-143, 2018.

H. Nishikawa, On Hyperbolic Method for Diffusion with Discontinuous Coefficients, Journal of Computational Physics, Volume 367, pp. 102-108, 2018.

List of Conference Papers (12)

Lingquan Li, Jialin Lou, Hong Luo, and Hiroaki Nishikawa, High-Order Hyperbolic Navier-Stokes Reconstructed Discontinuous Galerkin Method for Unsteady Flows, AIAA 2019-3060, AIAA Aviation 2019 Forum, 17-21 June 2019, Dallas, Texas, 2019

Lingquan Li, Jialin Lou, Hong Luo, and Hiroaki Nishikawa, "High-Order Hyperbolic Navier-Stokes Reconstructed Discontinuous Galerkin Method", AIAA Paper 2019-1150, AIAA Scitech 2019 Forum, 7-11 January 2019, San Diego, California.

Jialin Lou and Lingquan Li and Hong Luo and Hiroaki Nishikawa, "Explicit Hyperbolic Reconstructed Discontinuous Galerkin Methods for Time-Dependent Problems", AIAA Paper 2018-4270, AIAA 2018 Fluid Dynamics Conference, 25-29 June 2018, Atlanta, Georgia.

Lingquan Li and Jialin Lou and Hong Luo and Hiroaki Nishikawa, "A New Formulation of Hyperbolic Navier-Stokes Solver based on Finite Volume Method on Arbitrary Grids", AIAA Paper 2018-4160, AIAA 2018 Fluid Dynamics Conference, 25-29 June 2018, Atlanta, Georgia.

Jialin Lou, Lingquan Li, Hong Luo, Hiroaki Nishikawa, "First-Order Hyperbolic System Based Reconstructed Discontinuous Galerkin Methods for Nonlinear Diffusion Equations on Unstructured Grids", AIAA Paper 2018-2094, 56th AIAA Aerospace Sciences Meeting, 8-12 January 2018, Kissimmee, Florida.

Lingquan Li, Xiaodong Liu, Jialin Lou, Hong Luo, Hiroaki Nishikawa, Yuxin Ren, "A Discontinuous Galerkin Method Based on Variational Reconstruction for Compressible Flows on Arbitrary Grids", AIAA Paper 2018-0831, 56th AIAA Aerospace Sciences Meeting, 8-12 January 2018, Kissimmee, Florida.

Hiroaki Nishikawa, "Uses of Zero and Negative Volume Elements for Node-Centered Edge-Based Discretization", AIAA Paper 2017-4295, 23rd AIAA Computational Fluid Dynamics Conference, 5 -9 June 2017, Denver, Colorado.

Jialin Lou, Lingquan Li, Xiaodong Liu, Hong Luo, Hiroaki Nishikawa, "Reconstructed Discontinuous Galerkin Methods Based on First-Order Hyperbolic System for Advection-Diffusion Equations", AIAA Paper 2017-3445, 23rd AIAA Computational Fluid Dynamics Conference, 5 -9 June 2017, Denver, Colorado.

Lingquan Li, Xiaodong Liu, Jialin Lou, Hong Luo, Hiroaki Nishikawa, Yuxin Ren, "A Finite Volume Method Based on Variational Reconstruction for Compressible Flows on Arbitrary Grids", AIAA Paper 2017-3097, 23rd AIAA Computational Fluid Dynamics Conference, 5 -9 June 2017, Denver, Colorado.

Jialin Lou and Xiaodong Liu and Hong Luo and Hiroaki Nishikawa, Reconstructed Discontinuous Galerkin Methods for Hyperbolic Diffusion Equations on Unstructured Grids, AIAA Paper 2017-0310, 55th AIAA Aerospace Sciences Meeting, 9 -13 January 2017, Grapevine, Texas.

H. Nishikawa and Y. Liu, Hyperbolic Navier-Stokes Method for High-Reynolds-Number Boundary Layer Flows, AIAA Paper 2017-0081, 55th AIAA Aerospace Sciences Meeting, 9-13 January 2017, Grapevine, Texas.

Jialin Lou, Hong Luo, and Hiroaki Nishikawa, Discontinuous Galerkin Methods for Hyperbolic Advection-Diffusion Equation on Unstructured Grids, The 9th International Conference on Computational Fluid Dynamics (ICCFD), July 11-15, Istanbul, Turkey, 2016.

Background and Motivations

The reconstructed Discontinuous Galerkin (rDG) methods [1, 2, 3, 4, 5, 6, 7, 8, 9, 10], originally developed by the NCSU team, have been successfully used for the simulation of inviscid, RANS, LES and DNS flows. This method is a natural choice for the solution of the hyperbolic equations, but far less certain for elliptic or parabolic problems such as the compressible Navier-Stokes (NS) equations, where diffusive viscous and heat fluxes exist.

On the other hand, a first-order hyperbolic system (FOHS) was developed [11, 12, 13, 14, 15, 16, 17, 18, 19, 20, 21] to reformulate the viscous terms. The FOHS method has been shown to offer several distinguished advantages over other viscous methods. This method leads to numerical schemes that can achieve the same order of accuracy in the solution and the derivative quantities. Moreover, it enables high quality derivative prediction on fully irregular grids. This capability has a critical importance to high-order viscous simulations over complex geometries for which grids are likely to be highly irregular and it is widely known that significant amount of numerical noise is introduced in the derivatives estimated by reconstruction as typical in finite volume (FV) methods or even in those predicted by DG methods on irregular grids. Therefore, the FOHS method has a potential for enabling fully arbitrary unstructured-grid generation and isotropic/anisotropic grid adaption built upon accurate high-order derivatives, thus promising a full potential of unstructured high-order methodologies for complex applications. Another advantage of the FOHS method lies in the construction of improved iterative solvers by a complete elimination of second-derivatives in the target partial differential equations (PDE), leading to speed-up and robustness. The implicit iterative solvers, as often required in implicit-time stepping schemes, are known to slow down for refined grids if the residual Jacobian is derived from inconsistent discretizations. The residual Jacobians,

or a preconditioner within a Newton-Krylov method, are often constructed based on a lower-order scheme, but inconsistent schemes are often used for viscous terms because first-order viscous schemes are not available. For the same reason, p-multigrid methods, which are popular in high-order methods, are not fully exploited for the potential. In the FOHS method, first-order viscous schemes can be constructed straightforwardly just like for any hyperbolic system, and therefore can provide consistent residual-Jacobians for implicit solvers and allow a full and systematic construction of p-multigrid methods. Finally, the FOHS method can improve not only the viscous discretization but also the inviscid discretization. As demonstrated in the previous papers [22, 23], high-order derivatives generated in the FOHS method can be used to improve the inviscid discretization.

The objective of the presented work is to develop a high-order unsteady viscous solver for 3D unstructured grids by combining the FOHS method and the rDG method. The developed method, i.e., hyperbolic Navier-Stokes with reconstructed Discontinuous Galerkin (HNS+rDG) method, is expected to bring several advancements: (1) reduction in computational cost and storage over DG methods; (2) high-order and accurate derivative predictions on irregular grids; (3) robust and systematic construction of iterative solvers; (4) high accuracy in the inviscid discretization. The capability of predicting derivative quantities on irregular grids is of critical importance to viscous flow simulations, especially for high-fidelity adaptive unstructured-grid simulations over complex geometries as well as complex grid structure such as moving overset grids. It is critical particularly because high-order methods are often used with grid-adaptation for practical purpose. The significance of this work lies in the new way of treating the viscous terms in high-order and accurate gradient prediction on unstructured grids, and inviscid discretization improvement via the viscous discretization.

Research Activities

Task 1: Develop the Hyperbolic rDG Method for Linear Advection-Diffusion Equations

High-order reconstructed discontinuous Galerkin methods based on FOHS for advection-diffusion equations are developed at first. The FOHS formulation allows a straightforward DG discretization for diffusion. Additional gradients introduced to form a hyperbolic system are used to reduce the total number of degrees of freedom, such that a $\mathrm{P_k}$ hyperbolic DG scheme is almost equivalent to a conventional $\mathrm{P_{k+1}}$ DG scheme in terms of accuracy. The cost is further reduced by means of the rDG method, where the highest order terms in the polynomials are obtained by gradient reconstruction process. The study shows that the variational reconstruction method yields more stable and accurate results than the least-squares method.

Basic Construction of Hyperbolic rDG Method

Consider a steady model advection-diffusion equation:

$$\frac{\partial \varphi}{\partial \tau} + a\frac{\partial \varphi}{\partial x} + b\frac{\partial \varphi}{\partial y} = \nu\left(\frac{\partial^2 \varphi}{\partial x^2} + \frac{\partial^2 \varphi}{\partial y^2}\right), \tag{1}$$

where τ is a pseudotime variable, (a, b) is a constant advection vector, and ν is a constant diffusion coefficient. In the FOHS method, the advection-diffusion equation is reformulated as

$$\frac{\partial \mathbf{U}}{\partial \tau} + \frac{\partial \mathbf{F}_x}{\partial x} + \frac{\partial \mathbf{F}_y}{\partial y} = \mathbf{S}, \tag{2}$$

where

$$\mathbf{U} = \begin{pmatrix} \varphi \\ u \\ v \end{pmatrix}, \qquad \mathbf{F}_x = \begin{pmatrix} a\varphi - \nu u \\ -\varphi/T_r \\ 0 \end{pmatrix}, \qquad \mathbf{F}_y = \begin{pmatrix} b\varphi - \nu v \\ 0 \\ -\varphi/T_r \end{pmatrix}, \qquad \mathbf{S} = \begin{pmatrix} f(x,y) \\ -u/T_r \\ -v/T_r \end{pmatrix}, \tag{3}$$

where u and v are called the gradient variables since they correspond to the solution gradient in the pseudo steady state, and T_r is a relaxation time suitably defined as described in Ref.[24]. This system is hyperbolic in τ, and therefore can be discretized by methods for hyperbolic systems. In this work, an upwind discretization is always employed [22].

To discretize it, we first define solution polynomials within each cell:

$$\mathbf{U}_h(x,y) = \mathbf{C}(x,y)\mathbf{V}(t), \tag{4}$$

where $\mathbf{C}$ is a basis matrix, and $\mathbf{V}$ is a vector of unknown polynomial coefficients. Then, following the standard Galerkin formulation, we obtain

$$\mathbf{M}\frac{d\mathbf{V}}{dt} = \mathbf{R}(\mathbf{V}), \tag{5}$$

where $\mathbf{M}$ is the mass matrix,

$$\mathbf{M} = \int_{\Omega_e} \mathbf{C}^T\mathbf{C}d\Omega, \tag{6}$$

and $\mathbf{R}$ is the residual vector, defined as

$$\mathbf{R} = \int_{\Omega_e} \frac{\partial \mathbf{C}^T}{\partial x_k}\mathbf{F}_k + \mathbf{C}^T S d\Omega - \int_{\Gamma_e} \mathbf{C}^T\mathbf{F}_k\mathbf{n}_k d\Gamma, \tag{7}$$

where $\mathbf{n}_k$ the unit outward normal vector to the Γ_e, the boundary of Ω_e.

The numerical polynomial solutions are represented using a Taylor series expansion at the cell center and normalized to improve the conditioning of

the system matrix wth the basis functions:

$$B_1 = 1, B_2 = \frac{x - x_c}{\triangle x}, B_3 = \frac{y - y_c}{\triangle y},$$

$$B_4 = \frac{1}{2}\left(B_2^2 - \frac{1}{\Omega_e}\int_{\Omega_e} B_2^2 d\Omega\right), B_5 = \frac{1}{2}\left(B_3^2 - \frac{1}{\Omega_e}\int_{\Omega_e} B_3^2 d\Omega\right),$$

$$B_6 = B_2 B_3 - \frac{1}{\Omega_e}\int_{\Omega_e} B_2 B_3 d\Omega,$$

$$B_7 = \frac{1}{6}\left(B_2^3 - \frac{1}{\Omega_e}\int_{\Omega_e} B_2^3 d\Omega\right), B_8 = \frac{1}{6}\left(B_3^3 - \frac{1}{\Omega_e}\int_{\Omega_e} B_3^3 d\Omega\right),$$

$$B_9 = \frac{1}{2}\left(B_2^2 B_3 - \frac{1}{\Omega_e}\int_{\Omega_e} B_2^2 B_3 d\Omega\right), B_{10} = \frac{1}{2}\left(B_2 B_3^2 - \frac{1}{\Omega_e}\int_{\Omega_e} B_2 B_3^2 d\Omega\right). \tag{8}$$

Unlike the conventional DG method, the FOHS method allows an efficient polynomial construction. For example, in the current model equation case, we need to define polynomials for three variables, φ, u, and v. However, the vector (u, v) corresponds to the solution gradient, and therefore we can define

$$\mathbf{U}_h(x, y) = \mathbf{CV} = \begin{pmatrix} B_1 & B_2 & B_3 \\ 0 & B_1 & 0 \\ 0 & 0 & B_1 \end{pmatrix} \begin{pmatrix} \varphi \\ u \\ v \end{pmatrix}, \tag{9}$$

which is a linear polynomial for φ and constant approximations to u and v. This particular discretization is called DG(P0P1)+DG(P0), where the former indicates the order of discretization for the primal variable φ and the latter indicates that for the gradient variables. The scheme is further improved by the rDG method, where these polynomials are made one-order higher by using reconstructed derivatives:

$$\mathbf{U}_h(x, y) = \mathbf{CV} = \begin{pmatrix} B_1 & B_2 & B_3 & B_4 & B_5 & B_6 \\ 0 & B_1 & 0 & B_2 & 0 & B_3 \\ 0 & 0 & B_1 & 0 & B_3 & B_2 \end{pmatrix} \begin{pmatrix} \varphi \\ u \\ v \\ \tilde{u}_x \\ \tilde{v}_y \\ \tilde{V}_{xy} \end{pmatrix}, \tag{10}$$

where the tilde indicates the reconstruction, e.g., a least-squares (LS) reconstruction or the variational reconstruction (VR) [10], which is an implicit

gradient method and is more stable than the LS method. Note that $\tilde{u}_x$, $\tilde{v}_y$, and $\tilde{V}_{xy}$ are reconstructed derivatives u_x, v_y, u_y (or v_x), respectively. In this case, we still keep three unknowns φ, u, and v, since others are reconstructed from them. This method is called DG(P0P2)+rDG_LS(P0P1) if the LS is used for the reconstruction or DG(P0P2)+rDG_VR(P0P1) if the VR method is used for the reconstruction. The developed hyperbolic rDG scheme is more efficient than the DG method since it achieves third-order accuracy in the advection term with only three unknowns, whereas the third-order conventional DG method requires a quadratic polynomial with six unknowns. This efficient construction can be systematically extended to higher-order schemes. This is the core idea and a fundamental advantage of the hyperbolic rDG method. In the following, we will present and discuss numerical results obtained with the hyperbolic rDG schemes.

2D Steady Advection Diffusion Problem

A steady model advection diffusion problem in a unit square domain is considered, i.e.,

$$\frac{\partial \varphi}{\partial \tau} + a\frac{\partial \varphi}{\partial x} + b\frac{\partial \varphi}{\partial y} = \nu\left(\frac{\partial^2 \varphi}{\partial x^2} + \frac{\partial^2 \varphi}{\partial y^2}\right). \tag{11}$$

The exact solution can be found accordingly. Three sets of grids, as shown in Fig.1, are considered to test the performance of the hyperbolic rDG methods.

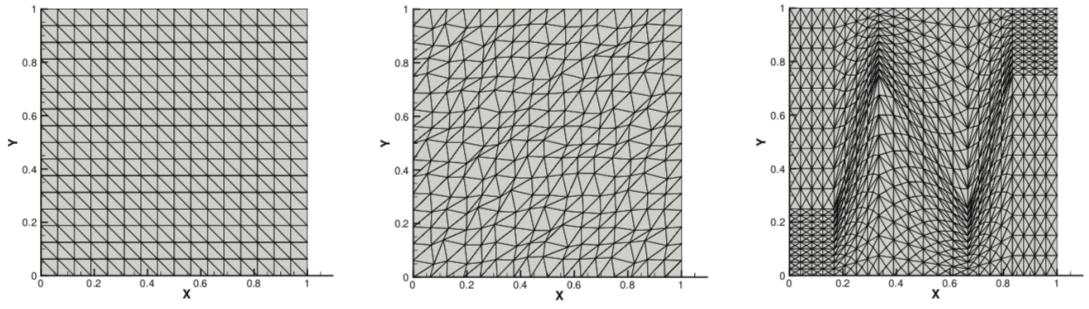

(a) 17×17 regular grid (b) 17×17 irregular grid (c) 23×21 heterogeneous grid

Figure 1: The sample grid of each type for 2D steady advection diffusion problem

Table 1: Order of accuracy on regular grids with different ν.

Scheme [DoFs]	Advection		Advection-Diffusion		Diffusion	
	φ	v_x	φ	v_x	φ	v_x
DG(P_0P_1)+DG(P_0) [3]	2.11	0 .99	1.26	1.00	1.95	1.00
DG(P_0P_2)+DG(P_1) [6]	3.02	2.01	2.03	1.62	2.05	1.62
DG(P_0P_3)+DG(P_2) [10]	3.97	2.97	3.65	2.99	3.59	2.97
DG(P_0P_2)+rDG_LS(P_0P_1) [3]	3.18	2.01	-	-	-	-
DG(P_0P_3)+rDG_LS(P_1P_2) [6]	4.14	3.22	3.69	2.82	3.70	2.82
DG(P_0P_2)+rDG_VR(P_0P_1) [3]	3.11	2.00	2.88	2.17	2.88	2.18
DG(P_0P_3)+rDG_VR(P_0P_2) [3]	4.49	3.28	3.04	2.90	2.99	2.81
DG(P_0P_3)+rDG_VR(P_1P_2) [6]	4.30	3.06	3.74	3.12	3.76	3.11

Table 2: Order of accuracy on irregular grids with different ν.

Scheme [DoFs]	Advection		Advection-Diffusion		Diffusion	
	φ	v_x	φ	v_x	φ	v_x
G(P_0P_1)+DG(P_0) [3]	1.93	0.99	1.26	0.92	1.92	0.89
DG(P_0P_2)+DG(P_1) [6]	2.74	1.91	2.38	1.73	2.39	1.73
DG(P_0P_3)+DG(P_2) [10]	3.97	2.97	2.99	2.72	2.96	2.75
DG(P_0P_2)+rDG_LS(P_0P_1) [3]	2.80	1.92	-	-	-	-
DG(P_0P_3)+rDG_LS(P_1P_2) [6]	4.18	3.19	3.61	2.67	3.61	2.70
DG(P_0P_2)+rDG_VR(P_0P_1) [3]	2.74	1.93	2.78	2.21	2.81	2.22
DG(P_0P_3)+rDG_VR(P_0P_2) [3]	3.77	2.97	3.02	2.62	3.01	2.78
DG(P_0P_3)+rDG_VR(P_1P_2) [6]	3.87	3.01	3.97	3.23	3.94	3.22

Table 3: Order of accuracy on heterogeneous grids with different ν.

Scheme [DoFs]	Advection		Advection-Diffusion		Diffusion	
	φ	v_x	φ	v_x	φ	v_x
DG(P_0P_1)+DG(P_0) [3]	2.11	0.95	1.17	1.00	1.98	1.00
DG(P_0P_2)+DG(P_1) [6]	3.15	2.07	2.60	1.92	2.60	1.92
DG(P_0P_3)+DG(P_2) [10]	4.08	3.04	3.12	2.76	3.10	2.76
DG(P_0P_2)+rDG_LS(P_0P_1) [3]	3.05	2.06	-	-	-	-
DG(P_0P_3)+rDG_LS(P_1P_2) [6]	4.17	3.11	3.87	2.99	4.00	3.10
DG(P_0P_2)+rDG_VR(P_0P_1) [3]	3.05	2.06	2.38	2.01	2.39	2.21
DG(P_0P_3)+rDG_VR(P_0P_2) [3]	4.51	3.27	3.57	3.09	3.53	3.04
DG(P_0P_3)+rDG_VR(P_1P_2) [6]	4.23	3.08	3.89	3.11	3.86	2.99

The accuracy and convergence of the hyperbolic rDG methods are shown in Tab.1, Tab.2 and Tab.3 for regular, irregular, and heterogeneous grids, respectively. Overall, the hyperbolic rDG methods are able to deliver the

designed or higher order of accuracy for most of the cases. All schemes converged without any problem in the advection limit. However, we do observe that DG(P_0P_2)+rDG(P_0P_1)_LS being unstable for non-advection limit cases. It appears that this issue can be fixed by either adding more cells in the LS stencils or applying limiters. On the other hand, DG(P_0P_3)+rDG(P_1P_2)_LS, DG(P_0P_3)+rDG(P_0P_2)_VR and DG(P_0P_3)+rDG(P_1P_2)_VR are stable. Variational reconstruction is based on a global stencil with compact data structure, resolving the stability issue of the LS reconstruction and thus making the extension to higher-order reconstruction simple and straightforward.

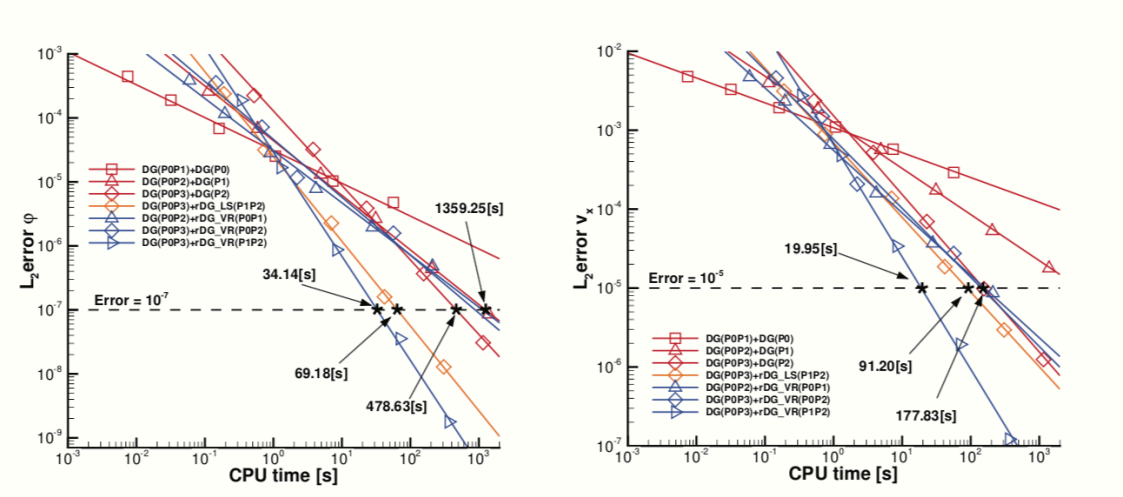

(a) L2 error of φ (b) L2 error of v_x

Figure 2: Efficiency plots of the hyperbolic rDG methods: Error versus CPU time for a sequence of 6 irregular grids with $\nu = 1, \mathrm{Re} = \sqrt{5}$.

The efficiency plots are shown in Fig.2, from where one can observe that for the same error, 10^{-7} in primary variable φ and 10^{-5} in the gradients, the presented rDG methods are more efficient than their DG counterparts. The DG(P_0P_3)+rDG(P_1P_2)_VR is the most efficient method as expected. The high efficiency of the VR based rDG methods is attributed to the fact that only one SGS relaxation sweep is used to solve the global linear system in the varational reconstruction at each time step and the convergence is only achieved at the steady state. The numerical results indicate that the presented hyperbolic rDG schemes with the variational reconstruction are attractive and worth further investigation.

2D Unsteady Advection Diffusion Problem

A 2D unsteady case is considered here. The analytical solution is given as

$$\varphi(x,y,t) = \frac{1}{4t+1} exp\left(-\frac{(x-at-x_0)^2+(y-bt-y_0)^2}{\nu(4t+1)}\right), \quad (x,y) \in [0,2]\times[0,2], \tag{12}$$

where

$$x_0 = y_0 = 1.0, \quad a = b = 10^{-5}, \nu = 0.01. \tag{13}$$

The regular and irregular grids of the 2D steady case are used with a scaling factor of 2. The physical time step is taken as $\Delta t = 10^{-3}$ with $t_{end} = 1$. For time integration, the third-order TVD-RK explicit time-stepping scheme was employed [**?**]. The time is here too small to impact the order of error convergence in grid refinement. The presented schemes are shown to provide the designed or higher order of accuracy in this unsteady case, as shown in Tab.4.

Table 4: Order of accuracy on 2D unsteady advection diffusion problem.

Scheme [DoFs]	Regular		Irregular	
	φ	v_x	φ	v_x
DG(P_0P_1)+DG(P_0) [3]	0.97	0.79	0.99	0.80
DG(P_0P_2)+DG(P_1) [6]	1.96	1.86	1.84	1.68
DG(P_0P_2)+rDG_LS(P_0P_1) [3]	2.34	2.24	1.94	1.95
DG(P_0P_3)+rDG_LS(P_1P_2) [6]	3.96	3.34	3.93	3.18
DG(P_0P_2)+rDG_VR(P_0P_1) [3]	2.89	2.30	2.64	2.24
DG(P_0P_3)+rDG_VR(P_0P_2) [3]	5.30	4.57	4.38	4.57
DG(P_0P_3)+rDG_VR(P_1P_2) [6]	3.76	3.66	3.81	3.56
DG(P_0P_4)+rDG_VR(P_1P_3) [6]	5.14	5.06	4.74	4.62

Task 2: Develop the HNS Method for Steady Compressible Viscous Flow Simulation

A New Hyperbolic Navier-Stokes System: HNS20G

In order to construct a hyperbolic rDG scheme for the Navier-Stokes equations, it was necessary to develop a new hyperbolic system with the gradients

of the primitive variables as additional variables, instead of those scaled by the viscosity as in the previous work [25, 26]. In this way, higher-order derivatives of the primitive variables can be easily obtained from the extra variables and their derivatives to build high-order polynomials of the primitive variables. To this end, we have developed the hyperbolic Navier-Stokes system called HNS20G [23]:

$$\mathbf{P}^{-1}\frac{\partial \mathbf{U}}{\partial \tau} + \mathbf{T}\frac{\partial \mathbf{U}}{\partial t} + \frac{\partial \mathbf{F}_k}{\partial x_k} = \mathbf{S}, \tag{14}$$

where τ refers to pseudo-time,

$$\mathbf{P}^{-1} = \begin{pmatrix} \begin{pmatrix} 1 & & \\ & \ddots & \\ & & 1 \end{pmatrix}_{5\times5} & & & & \\ & \begin{pmatrix} T_v & & \\ & \ddots & \\ & & T_v \end{pmatrix}_{9\times9} & & & \\ & & \begin{pmatrix} T_h & & \\ & \ddots & \\ & & T_h \end{pmatrix}_{3\times3} & & \\ & & & \begin{pmatrix} T_r & & \\ & \ddots & \\ & & T_r \end{pmatrix}_{3\times3} \end{pmatrix}, \tag{15}$$

$$\mathbf{T} = \begin{pmatrix} \begin{pmatrix} 1 & & \\ & \ddots & \\ & & 1 \end{pmatrix}_{5\times5} & \\ & \begin{pmatrix} 0 & & \\ & \ddots & \\ & & 0 \end{pmatrix}_{15\times15} \end{pmatrix}. \tag{16}$$

and $\mathbf{U}$ and $\mathbf{S}$ are defined as

$$\mathbf{U} = \left(\rho, \quad \rho u, \quad \rho v, \quad \rho w, \quad \rho e, \quad \mathbf{g}_u^T, \quad \mathbf{g}_v^T, \quad \mathbf{g}_w^T, \quad \mathbf{h}^T, \quad \mathbf{r}^T\right)^T, \tag{17}$$

$$\mathbf{S} = \left(0, \quad 0, \quad 0, \quad 0, \quad 0, \quad -\mathbf{g}_u^T, \quad -\mathbf{g}_v^T, \quad -\mathbf{g}_w^T, \quad -\mathbf{h}^T, \quad -\mathbf{r}^T\right)^T, \tag{18}$$

with the superscript T to denote the transpose, and the gradient variables:

$$\begin{aligned}
\mathbf{r} = \nabla\rho = \begin{pmatrix} \rho_x \\ \rho_y \\ \rho_z \end{pmatrix}, \quad \mathbf{g}_u = \nabla u = \begin{pmatrix} u_x \\ u_y \\ u_z \end{pmatrix}, \quad \mathbf{g}_v = \nabla v = \begin{pmatrix} v_x \\ v_y \\ v_z \end{pmatrix}, \\
\mathbf{g}_w = \nabla w = \begin{pmatrix} w_x \\ w_y \\ w_z \end{pmatrix}, \quad \mathbf{h} = \nabla T = \begin{pmatrix} T_x \\ T_y \\ T_z \end{pmatrix},
\end{aligned} \tag{19}$$

where ρ is the density, (u, v, w) is the velocity vector, T is the temperature, and the subscript indicates the derivative.

To discretize it, we define local polynomials for the primitive variables and apply the weak formulation to the HNS20G system written in the form:

$$\mathbf{P^{-1}}\frac{\partial \mathbf{U}}{\partial \mathbf{W}}\frac{\partial \mathbf{W}}{\partial \tau} + \mathbf{T}\frac{\partial \mathbf{U}}{\partial \mathbf{W}}\frac{\partial \mathbf{W}}{\partial t} + \frac{\partial \mathbf{F}_k}{\partial x_k} = \mathbf{S}, \tag{20}$$

where

$$\mathbf{W} = [\rho, u, v, w, T, \mathbf{g}_u^T, \quad \mathbf{g}_v^T, \quad \mathbf{g}_w^T, \quad \mathbf{h}^T, \quad \mathbf{r}^T]^T. \tag{21}$$

The polynomials of the primitive variables can be made higher-order by adding higher-order terms expressed in terms of higher-order derivatives of the gradient variables: e.g., for the density,

$$\begin{pmatrix} \rho^R \\ r_x^R \\ r_y^R \\ r_z^R \end{pmatrix} = \begin{pmatrix} B_1 & B_2 & B_3 & B_4 \\ & \frac{1}{\Delta x} & & \\ & & \frac{1}{\Delta y} & \\ & & & \frac{1}{\Delta z} \end{pmatrix} \begin{pmatrix} \overline{\rho} \\ \Delta x \overline{r}_x \\ \Delta y \overline{r}_y \\ \Delta z \overline{r}_z \end{pmatrix}, \tag{22}$$

where

$$B_1 = 1, \quad B_2 = \frac{x - x_c}{\Delta x}, \quad B_3 = \frac{y - y_c}{\Delta y}, \quad B_4 = \frac{z - z_c}{\Delta z}. \tag{23}$$

In this way, we only store and compute $\overline{\rho}$ for the density and its gradient is directly evaluated by the gradient variables $(\overline{r}_x, \overline{r}_y, \overline{r}_z)$. These polynomials are made even higher-order by using reconstructed derivatives as described for the model equations. As a result, we have developed HNS(P_0P_1+P_0), HNS(P_0P_2+P_0P_1_VR), HNS(P_0P_3+P_0P_2_VR) methods. Further details can be found in Refs.[23, 27, 28]. For steady problems, the implicit defect-correction solver is employed as described in Refs.[23, 27]. For unsteady problems, the ESDIRK implicit time-stepping scheme is employed as described in Ref.[28]

2D Manufactured Problem

A 2D manufactured problem is introduced to verify the accuracy of the HNS+rFV method. The numerical experiment is executed on four types of grids. These four sets of grids are composed of regular hexahedral, regular prismatic, distorted prismatic and highly-skewed prismatic cells, respectively, as is shown in Fig. 3. The following functions are made the exact solutions by introducing source terms into the Navier-Stokes equations:

$$\begin{cases} \rho = 1.0 + 0.15 \cdot \sin(1.0 \cdot x + 2.0 \cdot y), \\ u = 0.3 + 0.16 \cdot \sin(2.5 \cdot x + 3.0 \cdot y), \\ v = 0.4 + 0.13 \cdot \sin(1.0 \cdot x + 3.0 \cdot y), \\ p = 1.62 + 0.31 \cdot \sin(3.0 \cdot x + 1.0 \cdot y). \end{cases} \tag{24}$$

A constant viscosity $\mu = \rho_{inf} v_{inf} L/Re$ is used here for a verification purpose. The subscript denotes the free stream values. The free stream state is taken as $\rho_{inf} = 1.0$ and $v_{inf} = 0.5$ here. The Reynolds number is taken as 10 and 10^5.

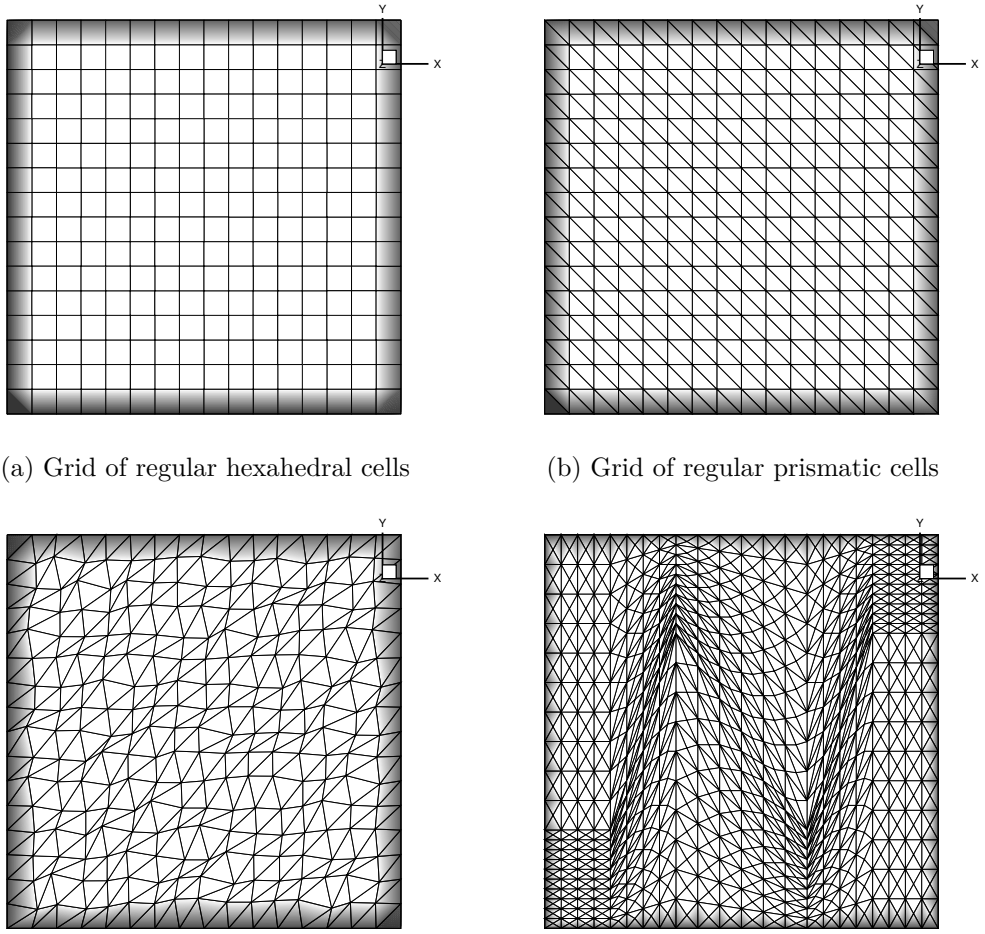

(a) Grid of regular hexahedral cells

(b) Grid of regular prismatic cells

(c) Grid of distorted hexahedral cells

(d) Grid of highly skewed hexahedral cells

Figure 3: Four types of prismatic mesh for 2D manufactured problem

The mesh convergence of Re = 10 and Re = 10^5 is shown in Fig.4 and Fig.5, respectively. For the viscous limit when Re = 10, all the primitive variables and auxiliary variables converge to first, second and third order of accuracy for HNS(P_0P_1+P_0), HNS(P_0P_2+P_0P_1_VR) and HNS(P_0P_3+P_0P_2_VR), respectively. However, when it comes to inviscid limit for Re = 10^5, the gradient variables still converge to first, second and third, but super-convergence occurs for primitive variables as they converge to second-, third- and forth-order of accuracy for these three methods, respectively.

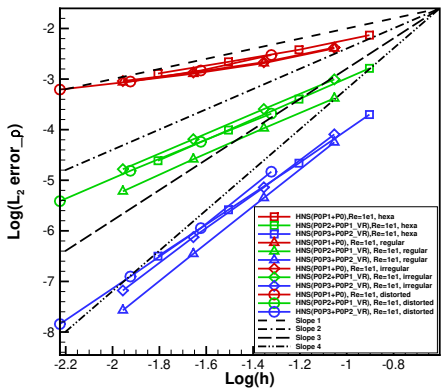

(a) Order of accuracy for density

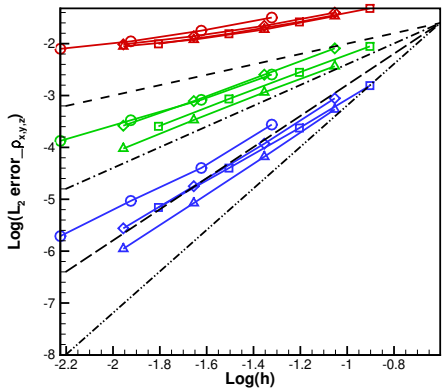

(b) Order of accuracy for the gradients of density

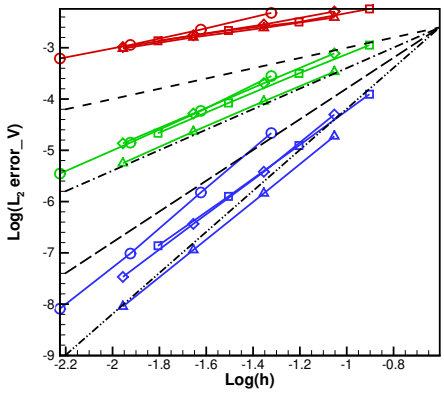

(c) Order of accuracy for velocity

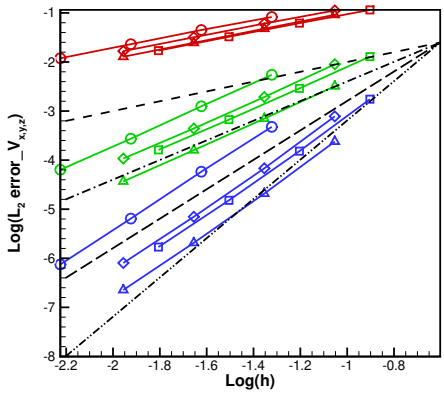

(d) Order of accuracy for the gradients of velocity

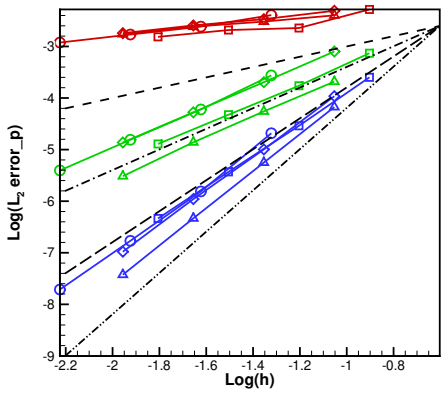

(e) Order of accuracy for pressure

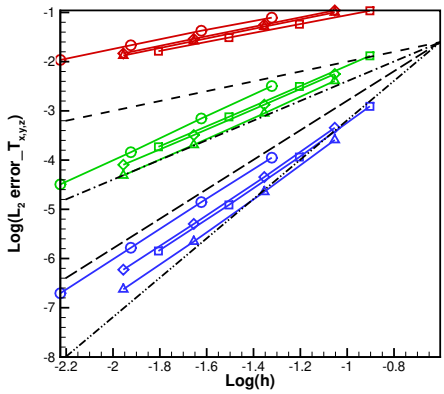

(f) Order of accuracy for the gradients of temperature

Figure 4: Mesh convergence of L2 error for manufactured solution, Re = 10

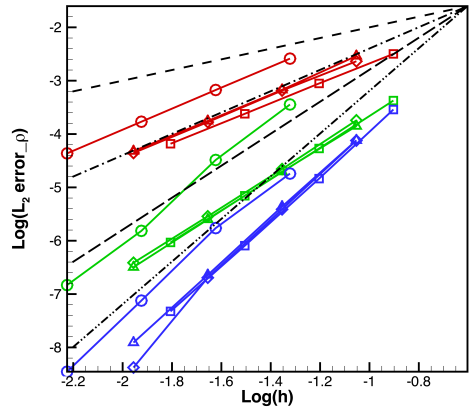

(a) Order of accuracy for density

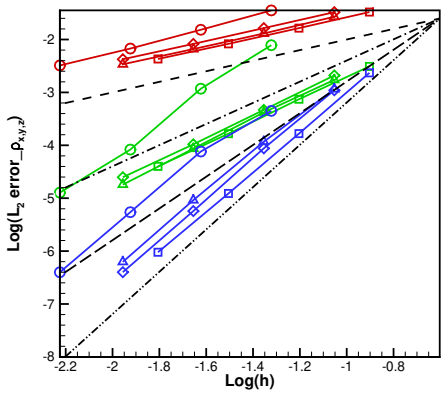

(b) Order of accuracy for the gradients of density

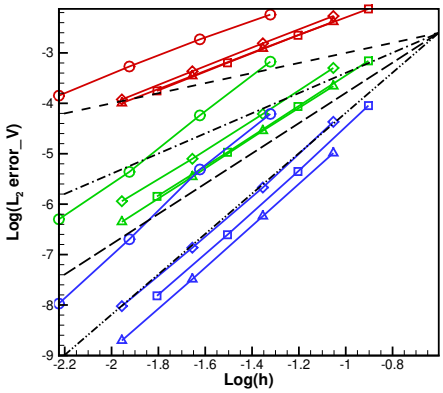

(c) Order of accuracy for velocity

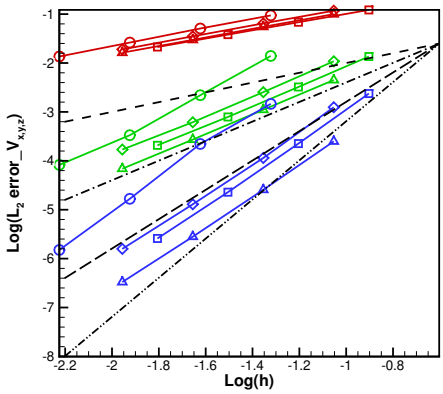

(d) Order of accuracy for the gradients of velocity

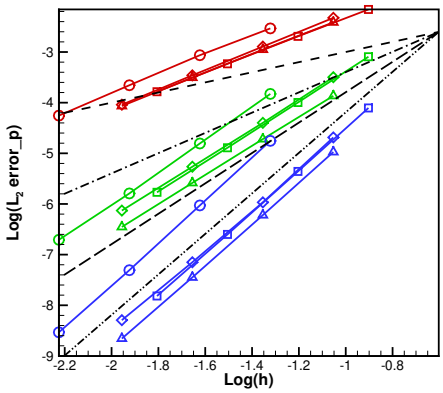

(e) Order of accuracy for pressure

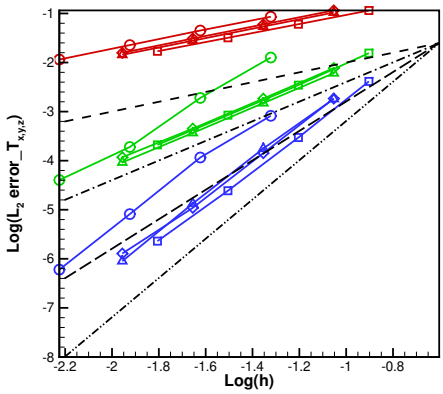

(f) Order of accuracy for the gradients of temperature

Figure 5: Mesh convergence of L2 error for manufactured solution, Re = 10^5

Laminar Flow Past a Flat Plate

The laminar boundary layer over an adiabatic flat plate at a free-stream Mach number of $M_\infty = 0.5$ and a Reynolds number of $\mathrm{Re} = 10^5$ based on the free-stream velocity and the length of the flat plate is considered here. This problem is chosen to illustrate the accuracy of the HNS methods, as the classical Blasius solution can be used to measure the accuracy of the numerical solution.

Computations are performed on a hexahedral grid, as is shown in Fig. 6. The computation domain is bounded from -0.5 to 1.0 along the x-direction, from 0 to 1.0 in the y-direction, and from 0 to 0.1 along the z-direction. The hexahedral grid used in this computation is composed of $(25 + 50) \times 1$ cells, with $25 \times 30 \times 1$ cells ahead of the flat plate and $50 \times 30 \times 1$ cells for the flat plate. In order to cluster points near the flat plate, the distribution of grid points in the y-direction follows a geometric stretching. The stretching ratio (SR) is taken as SR = 1.3 for the ratio of the heights of the two successive elements. The computation is performed with HNS($\mathrm{P_0P_1}$+$\mathrm{P_0P}$) and HNS($\mathrm{P_0P_2}$+$\mathrm{P_0P_1}$_VR) methods. The pressure contours near the front of the flat plate are shown in Fig.7. Fig 8 provides the logarithmic plot of the computed skin friction coefficient c_f distributions along the flat plat. The skin friction coefficient c_f is defined by

$$c_f = \frac{\tau_w}{\frac{1}{2}\rho u_\infty^2}, \tag{25}$$

where τ_w is the local wall shear stress

$$\tau_w = \mu \left(\frac{\partial u}{\partial y} \right)_{y=0}, \tag{26}$$

where μ is the dynamic viscosity, ρ is the fluid density and u_∞ is the free-stream velocity.

Fig. 9 shows the plot of velocity profiles versus similarity variable η for computed x-velocity u and scaled y-velocity v^+ along the cells cut through by plane of $x = 0.1$ and $x = 0.5$ in the boundary layer region. The similarity variable η is defined as

$$\eta = \frac{y}{\delta(x)} = \frac{y}{\sqrt{\frac{\nu x}{u_\infty}}}, \tag{27}$$

where $\delta(x)$ is the scaling argument, and x is the downstream coordinate. It can be observed from Fig.9 that the u profiles at both downstream lo-

cations match quite well with the analytical solution, which illustrates a consistent convergence and accuracy of the numerical HNS methods. On the other side, the v^+ profiles are also able to match the analytical solution, but not as good as the u profiles, since y-velocity is relatively a very small quantity with respect to x-velocity, and requires a much higher grid resolution if expected to match the analytical solution better. Moreover, the v^+ profile obtained with HNS(P_0P_2+P_0P_1_VR) method matches better than the other one of HNS(P_0P_1+P_0) method, demonstrating that the reconstructed HNS(P_0P_2+P_0P_1_VR) method is more accurate than the baseline HNS(P_0P_1+P_0) method.

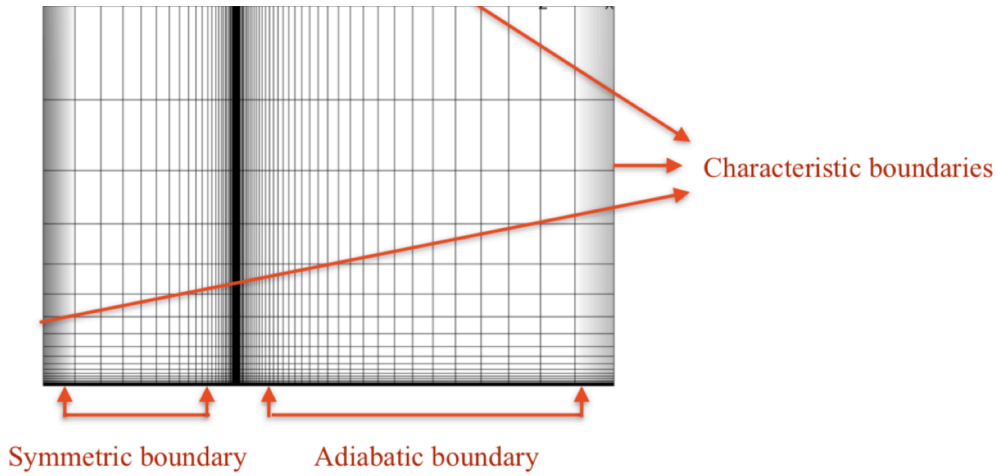

Figure 6: Plot of the hexahedral grid for laminar flow past a flat plat at $\mathrm{Re} = 10^5$

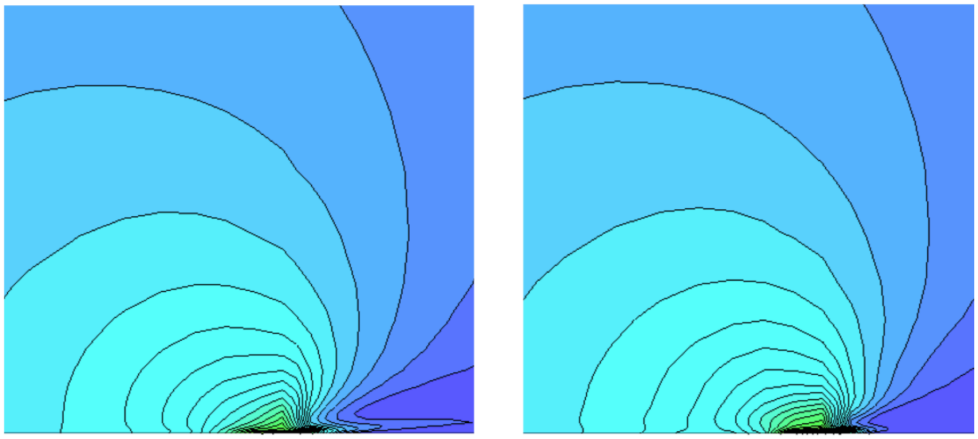

(a) HNS(P_0P_1+P_0) result (b) HNS(P_0P_2+P_0P_1_VR) result

Figure 7: Pressure contours obtained with HNS(P_0P_1+P_0) and HNS(P_0P_2+P_0P_1_VR) methods for laminar flow past a flat plate

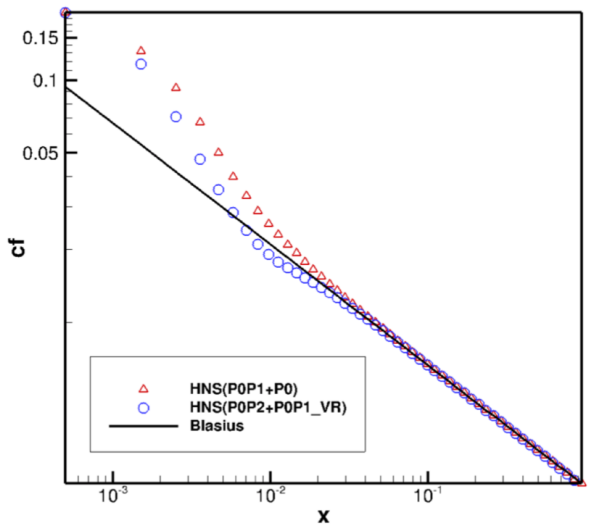

Figure 8: Logarithmic plot of the computed skin friction coefficient c_f distribution obtained with HNS(P_0P_1+P_0) and HNS(P_0P_2+P_0P_1_VR) methods compared with analytical solution along the flat plate $0 \leq x \leq 1$

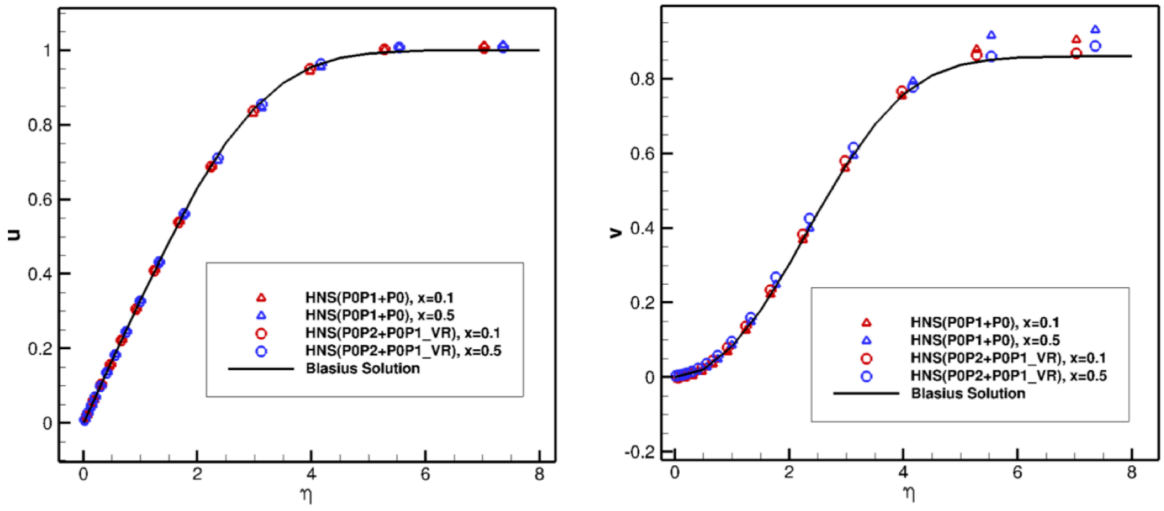

(a) x-velocity (b) y-velocity

Figure 9: Plot of velocity versus similarity variable η obtained with HNS(P_0P_1+P_0) and HNS(P_0P_2+P_0P_1_VR) methods and compared with the analytical solutions at downstream coordinates $x = 0.1$ and $x = 0.5$ in the boundary layer region

Laminar Flow Past a Sphere

The laminar flow past a sphere is simulated here to testify the accuracy of the rDG methods base on HNS20G equations. The grids are shown in Fig. 10.

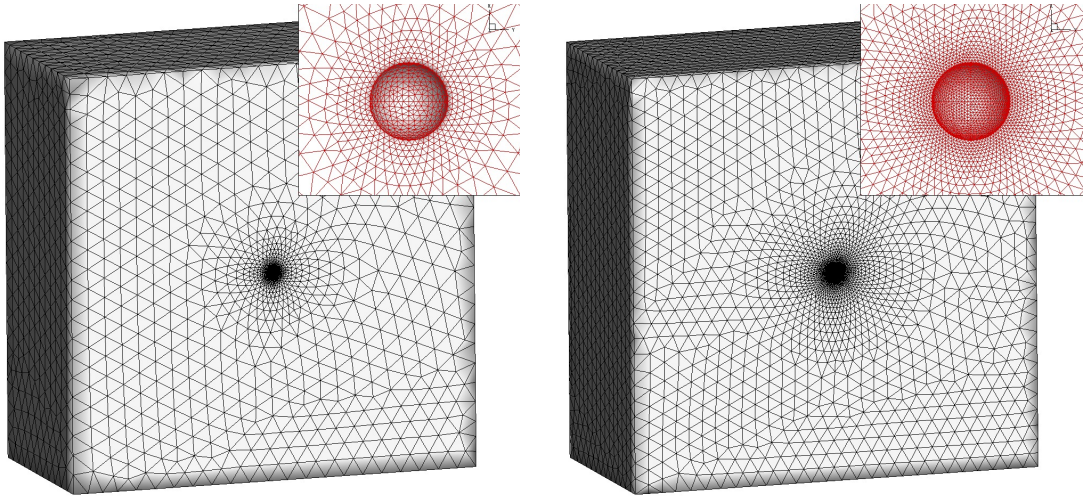

(a) Level 1 (b) Level 2

Figure 10: Tetrahedral grids for laminar flow past a sphere

We start with a free-stream Mach number of $M_\infty = 0.5$ and Reynold's number of Re = 100. The residuals' convergence of velocity and the gradients of velocity are compared between HNS(P_0P_1+P_0), HNS(P_0P_2+P_0P_1_VR) and DG(P_1) methods on the coarse grid in Fig.11, from where we can see that given the same convergence threshold of the linear solver at each step of Newton's method (the relative residual magnitude drops with one-order), HNS(P_0P_2+P_0P_1_VR) method converges faster than conventional DG(P_1) method to a steady-state, i.e., to a state where the residuals are small enough. This is expected because by implementing the HNS20G method, the second-order derivatives in the NS equations are eliminated. The Jacobian matrix for HNS(P_0P_2+P_0P_1_VR) method is not accurate anymore because of the fact that reconstruction techniques are involved. That's why HNS(P_0P_2+P_0P_1_VR) method converges slower to a steady-state than conventional DG(P_1) method in the presented work.

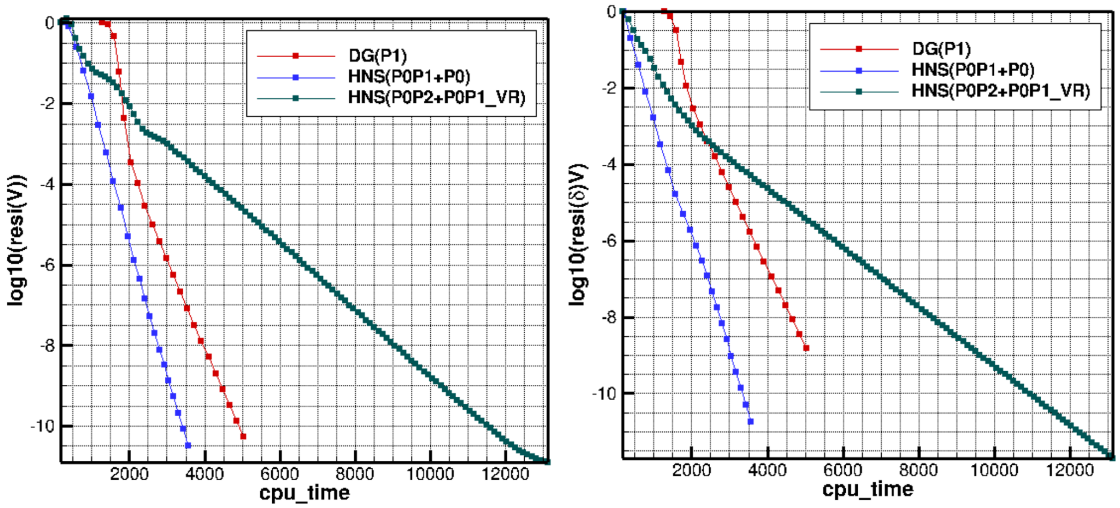

(a) Residuals of velocity (b) Residuals of the gradients of velocity

Figure 11: Convergence of the residuals of velocity and its gradients with HNS(P_0P_1+P_0), HNS(P_0P_2+P_0P_1_VR) and DG(P_1) methods for laminar flow past a sphere at $M_\infty = 0.5$ and Re = 100 on the coarse grid

The voricity magnitude contours are given in Fig.12, where HNS(P_0P_1+P_0) and DG(P_1) give the similar results, but HNS(P_0P_2+P_0P_1_VR) method gives a smoother result than HNS(P_0P_1+P_0) and DG(P_1) methods.

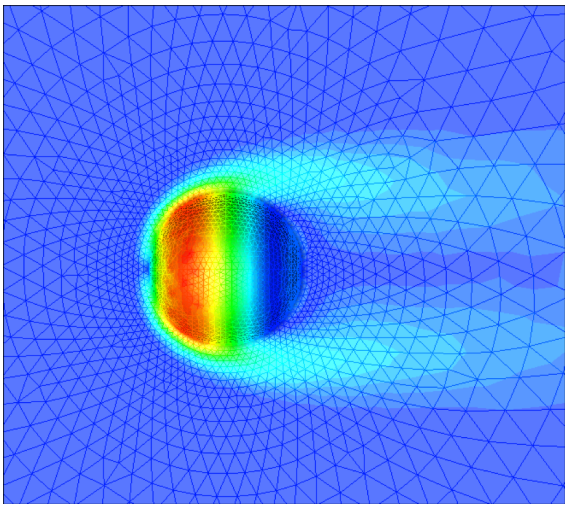

(a) DG(P_1)

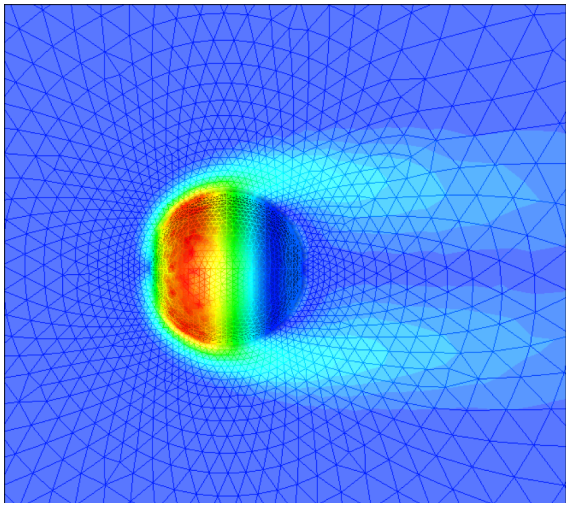

(b) HNS(P_0P_1+P_0)

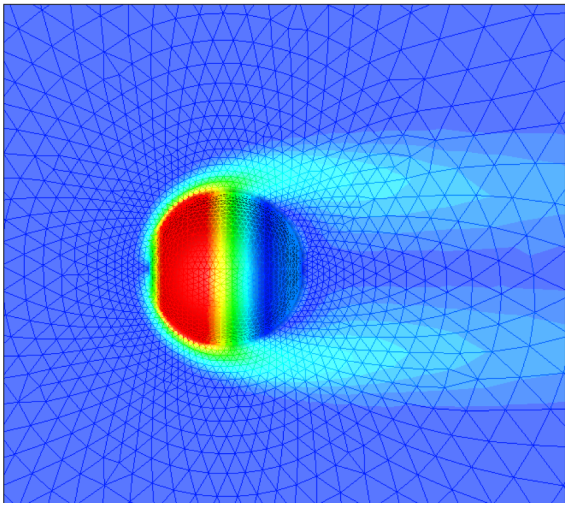

(c) HNS(P_0P_2+P_0P_1_VR)

Figure 12: Vorticity magnitude contours obtained with HNS(P_0P_1+P_0), HNS(P_0P_2+P_0P_1_VR) and DG(P_1) methods for laminar flow past a sphere at $M_\infty = 0.5$ and Re = 100 on the fine grid

The Reynold's number is then increased to Re = 250. The Mach contours and the streamlines obtained with HNS(P_0P_2+P_0P_1_VR) method on the fine mesh are given in Fig. 13, and compared with the reference solution [29]. The flow becomes asymmetric at this condition, but still laminar.

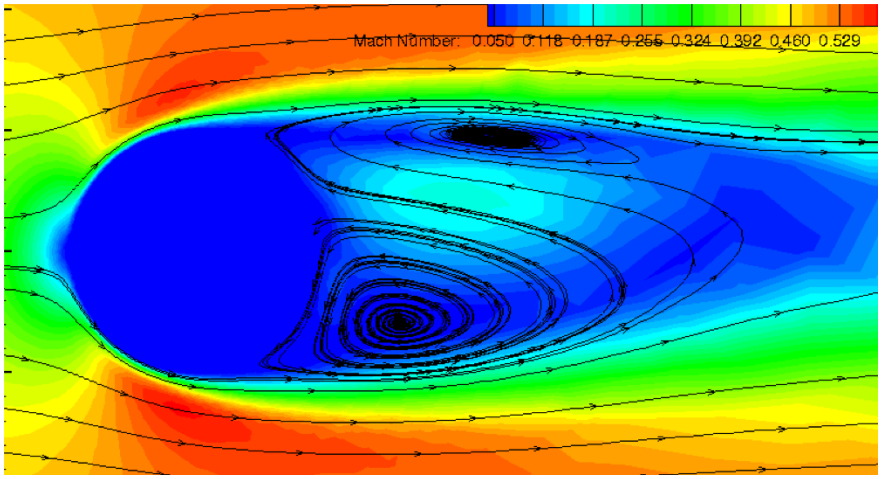

(a) HNS(P_0P_2+P_0P_1_VR)

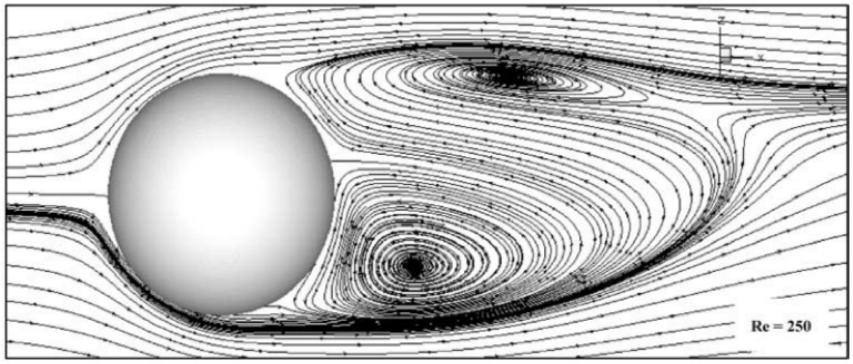

(b) Reference solution [29]

Figure 13: Mach number contours and streamlines obtained with HNS(P_0P_2+P_0P_1_VR) method for laminar flow past a sphere at $M_\infty = 0.5$ and Re = 250 on the fine grid and compared with reference solution

Laminar Flow Past a Delta Wing

A laminar flow at a high angle of attack past a delta wing with a sharp leading edge and a blunt trailing edge is considered here. The free stream Mach number is of $M_\infty = 0.3$, the angle of attack is $\alpha = 12.5^o$, and the Reynolds number is of Re $= 4,000$ based on a mean cord length of 1. The objective here is to assess if the rDG methods based on HNS20G equations are able to effectively resolve the flow features in more complex conditions. A tetrahedral grid consisting of $670,680$ tetrahedral elements, $197,752$ grid points and $25,944$ triangular boundary faces. The triangular meshes of the delta wing surface are illustrated in Fig. 14. The no-slip and adiabatic boundary conditions are prescribed to the wing surface. Both HNS(P_0P_1+P_0)

and HNS(P_0P_2+P_0P_1_VR) methods are used to perform the computation. The computed vorticity magnitude contours are displayed in Fig. 15 along with the stream-straces in the flow field. It is observed that as the flow passes the leading edge, it rolls up and creates a vortex together with a secondary vortex. The vortex system remains over a distance behind the wing.

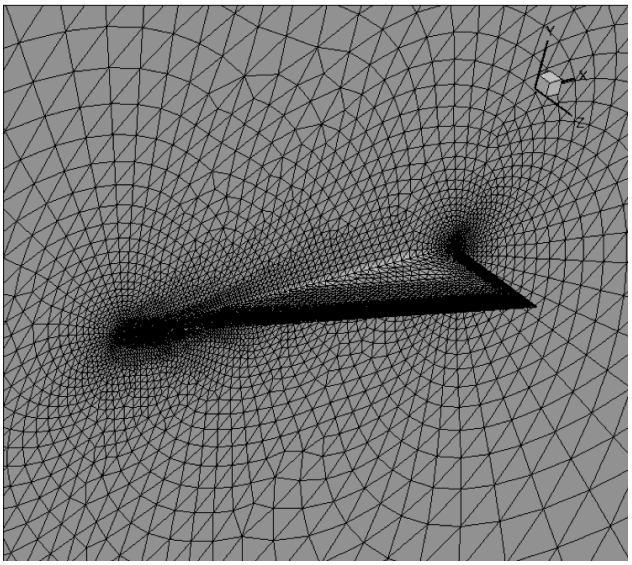

Figure 14: Tetrahedral grid used for laminar flow past a Delta wing

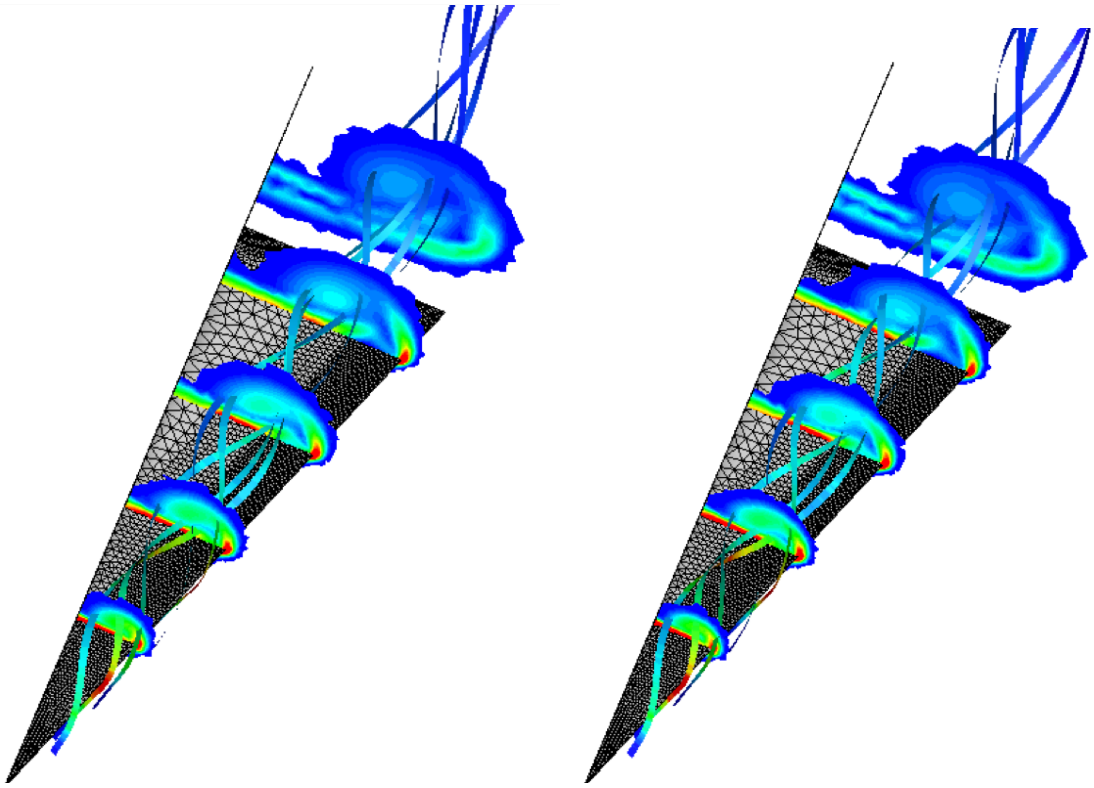

(a) HNS(P_0P_1+P_0) (b) HNS(P_0P_2+P_0P_1_VR)

Figure 15: Vorticity magnitude contours and stream-traces obtained with HNS(P_0P_1+P_0) and HNS(P_0P_2+P_0P_1_VR) methods for laminar flow past a Delta wing

Task 3: Develop the HNS Method for Unsteady Compressible Viscous Flow Simulation

Von-Karman Vortex Street Behind A Circular Cylinder

The von-Karman vortex street is one of the most extensively studied case both experimentally and numerically in fluid dynamics. The initial condition is a uniform free-stream with non-slip and adiabatic wall boundary on the circular cylinder surface. The free-stream Mach number is taken as $M_\infty = 0.1$ and the Reynold's number is taken as $\mathrm{Re} = 100$ based on the diameter of the cylinder. The grid is composed of $21,809$ prismatic elements, $22,804$ grid points $43,168$ triangular boundary faces and 199 quadratic boundary faces. The third-order ESDIRK method is used for time marching with a fixed physical-time step $\Delta t = 0.2$. The computation is performed with HNS(P_0P_2+P_0P_1_VR)

method. The drag and lift coefficients are reported in Fig. 17. The vorticity magnitude contours within one half period is shown in Fig. 18.

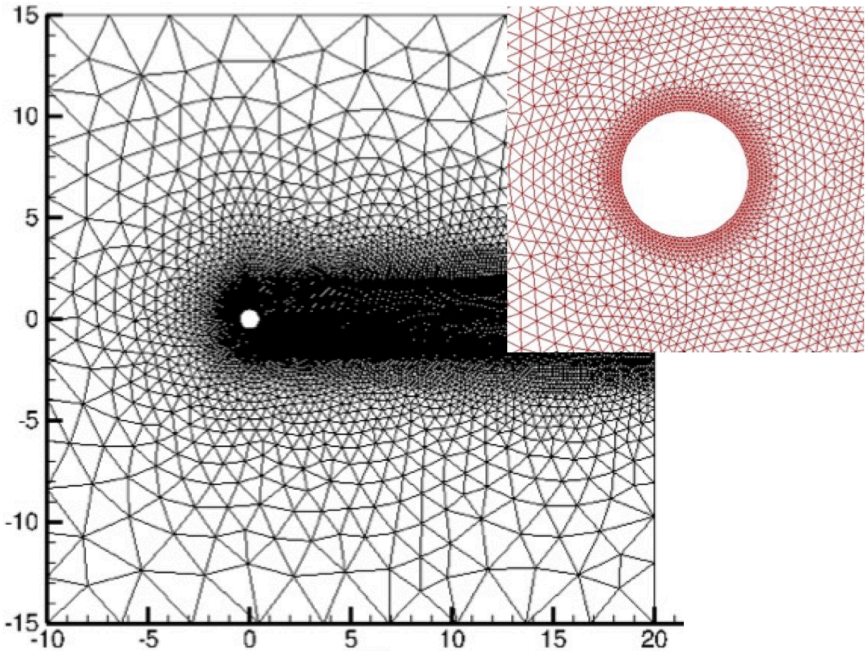

Figure 16: Prismatic grid used for von-Karman vortex street behind a circular cylinder

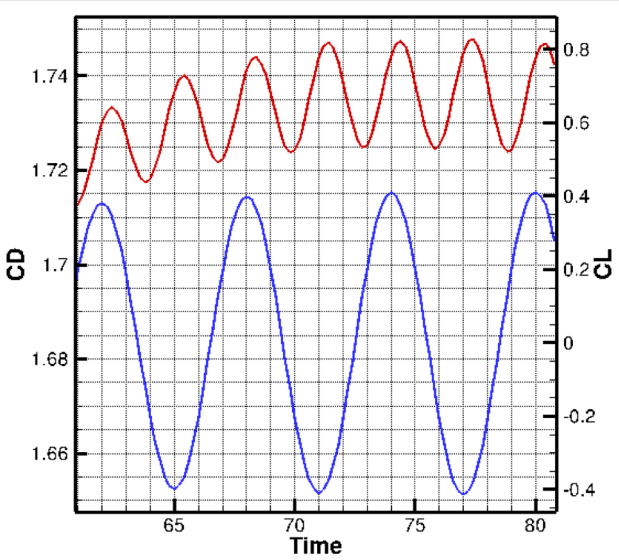

Figure 17: Time history of the computed lift and drag coefficient for von-Karman vortex street behind a circular cylinder at $N_\infty = 0.1$ and Re = 100 with HNS(P_0P_2+P_0P_1_VR) method

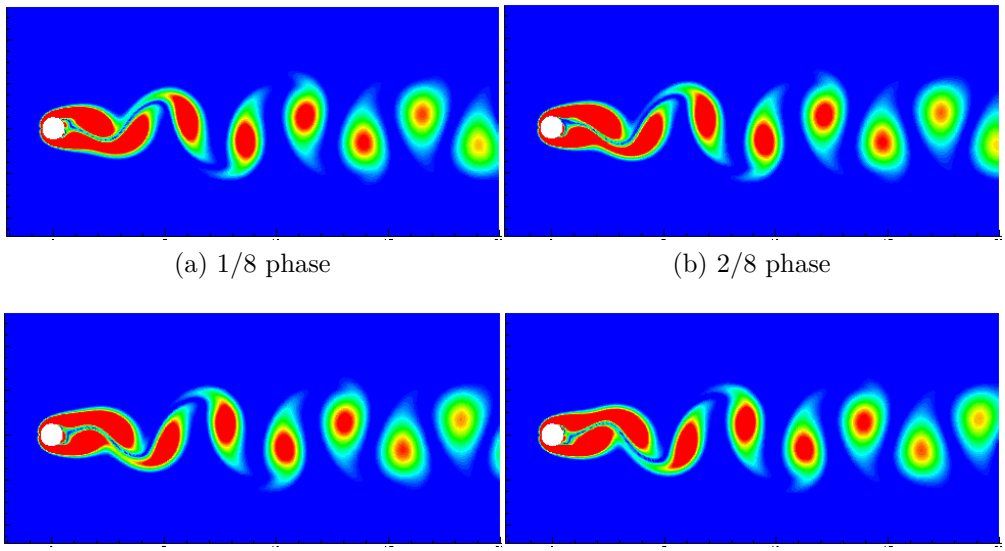

(a) 1/8 phase (b) 2/8 phase

(c) 3/8 phase (d) 4/8 phase

Figure 18: Vorticity magnitude contours at four phases within a half period for von-Karman vortex street behind a circular cylinder with HNS(P_0P_2+P_0P_1_VR) method

Concluding Remarks and Future Work

A new formulation of first-order hyperbolic Navier-Stokes equations, i.e., HNS20G is first derived. Different from previous works about HNS, the auxiliary variables in the HNS20G equations are taken directly as the gradients of density, velocity and temperature.

With this new HNS20G, a reconstruction strategy, namely variational reconstruction, is allowed to be taken into account for spatial discretization. Then, the auxiliary variables are recycled to get a higher-order polynomial estimation of the primitive variables, i.e., density, velocity and temperature. A higher-order estimation is obtained by performing a reconstruction strategy, variational reconstruction, on the gradient variables.

The HNS+rDG methods based on the newly developed HNS20G equations are implemented for numberical experiments. From the numerical results, we can see that the HNS method is efficient, accurate and robust. The HNS methods converge faster than DG(P_1) methods with the same number of degree of freedoms. The higher-order reconstructed HNS method converges slower. This is because that in the implicit time marching methods, although the Jacobian matrix is exact for the baseline HNS methods by using the automatic differentiation tool, the Jacobian matrix is not exact anymore when the variational reconstruction is used. However, the reconstructed method based on HNS20G equations gives a much smoother solution than the conventional DG counterpart with the same degree of freedom, demonstrating the high accuracy for the rDG methods based on the HNS20G equations. Finally, a numerical simulation of an unsteady Karmen-vortex is carried out with HNS+rDG method and ESDIRK time integration to show that the present method is able to solve for real unsteady flow problems.

It is noticeable that the HNS(P_0P_1+P_0) method is important and unique. This method is compact, efficient, and gives first-order of accuracy in the

gradients, while any conventional first-order viscous scheme will only give zeroth-order of accuracy in the gradients. This method is also accurate for many real flow problems as shown in this work.

The developed rDG+HNS methods showed their potential for future works. First, high-performance computing techniques can be implemented to optimize the performance of the presented schemes. Second, these methods can be extended to simulate real flows with high Reynold's number, or even turbulent flows. Third, because the baseline HNS methods are faster than conventional DG when it comes to convergence, and the high-order HNS methods are able to get more accurate results than DG methods, especially when it comes to the gradients, the presented methods can also be considered to be implemented with *hp*-adaptation, so that accurate results can be obtained without too much sacrifice of computing resources. The presented HNS methods are able to get accurate and noise-free velocity gradients even on highly distorted grids, which makes it suitable for *hp*-adaptation, where the grid will be highly irregular and the accuracy of the gradients becomes a great concern. Additionally, the superior gradient accuracy of HNS is a very strong advantage for enabling anisotropic grid adaptation through a boundary layer. It is an enabling feature for future adaptive-grid simulations since the current state-of-the-art methods cannot provide satisfactory accuracy in gradients on adaptive grids. As such, the next logical step would be to apply the HNS method to fully adaptive-grid simulations.

Bibliography

[1] Hong Luo, Luqing Luo, Amjad Ali, Robert Nourgaliev, and Chunpei Cai. A parallel, reconstructed discontinuous galerkin method for the compressible flows on arbitrary grids. *Communications in Computational Physics*, 9(2):363–389, 2011.

[2] Hong Luo, Joseph D Baum, and Rainald Löhner. A hermite weno-based limiter for discontinuous galerkin method on unstructured grids. *Journal of Computational Physics*, 225(1):686–713, 2007.

[3] Hong Luo, Yidong Xia, Shujie Li, Robert Nourgaliev, and Chunpei Cai. A hermite weno reconstruction-based discontinuous galerkin method for the euler equations on tetrahedral grids. *Journal of Computational Physics*, 231(16):5489–5503, 2012.

[4] Yidong Xia, Hong Luo, and Robert Nourgaliev. An implicit hermite weno reconstruction-based discontinuous galerkin method on tetrahedral grids. *Computers & Fluids*, 96:406–421, 2014.

[5] Hong Luo, Yidong Xia, Seth Spiegel, Robert Nourgaliev, and Zonglin Jiang. A reconstructed discontinuous galerkin method based on a hierarchical weno reconstruction for compressible flows on tetrahedral grids. *Journal of Computational Physics*, 236:477–492, 2013.

[6] Hong Luo, Luqing Luo, Robert Nourgaliev, Vincent A Mousseau, and Nam Dinh. A reconstructed discontinuous galerkin method for the compressible navier–stokes equations on arbitrary grids. *Journal of Computational Physics*, 229(19):6961–6978, 2010.

[7] Hong Luo, Luqing Luo, Robert Nourgaliev, and Vincent Mousseau. A reconstructed discontinuous galerkin method for the compressible euler equations on arbitrary grids. In *19th AIAA Computational Fluid Dynamics*, page 3788. 2009.

[8] Hong Luo, Yidong Xia, and Robert Nourgaliev. A class of reconstructed discontinuous galerkin methods in computational fluid dynamics. Technical report, Idaho National Laboratory (INL), 2011.

[9] Hong Luo, Hanping Xiao, Robert Nourgaliev, and Chumpei Cai. A comparative study of different reconstruction schemes for a reconstructed discontinuous galerkin method on arbitrary grids. In *20th AIAA Computational Fluid Dynamics Conference*, page 3839, 2011.

[10] Lingquan Li, Xiaodong Liu, Jialin Lou, Hong Luo, Hiroaki Nishikawa, and Yuxin Ren. A discontinuous galerkin method based on variational reconstruction for compressible flows on arbitrary grids. In *2018 AIAA Aerospace Sciences Meeting*, page 0831, 2018.

[11] Yi Liu and Hiroaki Nishikawa. Third-order inviscid and second-order hyperbolic navier-stokes schemes for three-dimensional inviscid and viscous flows. In *46th AIAA Fluid Dynamics Conference*, page 3969, 2016.

[12] Alireza Mazaheri and Hiroaki Nishikawa. Improved second-order hyperbolic residual-distribution scheme and its extension to third-order on arbitrary triangular grids. *Journal of Computational Physics*, 300:455–491, 2015.

[13] Yoshitaka Nakashima, Norihiko Watanabe, and Hiroaki Nishikawa. Hyperbolic navier-stokes solver for three-dimensional flows. In *54th AIAA Aerospace Sciences Meeting*, page 1101, 2016.

[14] Hiroaki Nishikawa. A first-order system approach for diffusion equation. i: Second-order residual-distribution schemes. *Journal of Computational Physics*, 227(1):315–352, 2007.

[15] Hiroaki Nishikawa. A first-order system approach for diffusion equation. ii: Unification of advection and diffusion. *Journal of Computational Physics*, 229(11):3989–4016, 2010.

[16] Hiroaki Nishikawa. First-, second-, and third-order finite-volume schemes for diffusion. *Journal of Computational Physics*, 256:791–805, 2014.

[17] Hiroaki Nishikawa. First, second, and third order finite-volume schemes for advection–diffusion. *Journal of Computational Physics*, 273:287–309, 2014.

[18] Hiroaki Nishikawa. Alternative formulations for first-, second-, and third-order hyperbolic navier-stokes schemes. In *22nd AIAA Computational Fluid Dynamics Conference*, page 2451, 2015.

[19] Hiroaki Nishikawa and Philip L Roe. Third-order active-flux scheme for advection diffusion: hyperbolic diffusion, boundary condition, and newton solver. *Computers & Fluids*, 125:71–81, 2016.

[20] Eleuterio F Toro and Gino I Montecinos. Advection-diffusion-reaction equations: hyperbolization and high-order ader discretizations. *SIAM Journal on Scientific Computing*, 36(5):A2423–A2457, 2014.

[21] Euntaek Lee, Hyung Taek Ahn, and Hong Luo. Cell-centered high-order hyperbolic finite volume method for diffusion equation on unstructured grids. *Journal of Computational Physics*, 355:464–491, 2018.

[22] Jialin Lou, Lingquan Li, Hong Luo, and Hiroaki Nishikawa. Reconstructed discontinuous galerkin methods for linear advection–diffusion equations based on first-order hyperbolic system. *Journal of Computational Physics*, 369:103–124, 2018.

[23] Lingquan Li, Jialin Lou, Hong Luo, and Hiroaki Nishikawa. A new formulation of hyperbolic navier-stokes solver based on finite volume method on arbitrary grids. In *2018 Fluid Dynamics Conference*, page 4160, 2018.

[24] Hiroaki Nishikawa and Yi Liu. Hyperbolic Navier-Stokes method for high-Reynolds-number boundary-layer flows. In *55th AIAA Aerospace Sciences Meeting*, AIAA Paper 2017-0081, Grapevine, Texas, 2017.

[25] Hiroaki Nishikawa. First, second, and third order finite-volume schemes for Navier-Stokes equations. In *Proc. of 7th AIAA Theoretical Fluid Mechanics Conference, AIAA Aviation and Aeronautics Forum and Exposition 2014*, AIAA Paper 2014-2091, Atlanta, GA, 2014.

[26] Hiroaki Nishikawa. Alternative formulations for first-, second-, and third-order hyperbolic Navier-Stokes schemes. In *Proc. of 22nd AIAA Computational Fluid Dynamics Conference*, AIAA Paper 2015-2451, Dallas, TX, 2015.

[27] Lingquan Li, Jialin Lou, Hong Luo, and Hiroaki Nishikawa. High-order hyperbolic navier-stokes reconstructed discontinuous galerkin method. In *AIAA Scitech 2019 Forum*, page 1150, 2019.

[28] Lingquan Li, Jialin Lou, Hong Luo, and Hiroaki Nishikawa. High-order hyperbolic navier-stokes reconstructed discontinuous galerkin method for unsteady flows. In *AIAA Aviation 2019 Forum*, page 3060, 2019.

[29] Anvar Gilmanov, F Sotiropoulos, and E Balaras. A general reconstruction algorithm for simulating flows with complex 3d immersed boundaries on cartesian grids. *Journal of Computational Physics*, 191(2):660–669, 2003.